*Biochemistry (Moscow), Vol. 70, No. 8, 2005, pp. 848-857. Translated from Biokhimiya, Vol. 70, No. 8, 2005, pp. 1030-1040.*

*Originally published in Biochemistry (Moscow) On-Line Papers in Press, as Manuscript BM04-048, February 20, 2005.*

# Effect of Mutation of the Conservative Glycine Residues Gly100 and Gly147 on Stability of *Escherichia coli* Inorganic Pyrophosphatase

**V. M. Moiseev[1]*, E. V. Rodina[1,2], and S. M. Avaeva[2]**

*[1]Faculty of Chemistry, Lomonosov Moscow State University, 119992 Moscow, Russia; fax: (7-095) 932-8846; E-mail: mbutt@mail.ru*
*[2]Belozersky Institute of Physico-Chemical Biology, Lomonosov Moscow State University, 119992 Moscow, Russia; fax: (7-095) 939-3181*

Received February 28, 2004
Revision received November 26, 2004

**Abstract**—Sequence alignment of inorganic pyrophosphatases (PPases) isolated from the different organisms shows that glycine residues Gly100 and Gly147 are conservative. These residues are located in flexible segments of a polypeptide chain that have similar structure in the different PPases. To elucidate the possible role of these segments in the functioning of PPase, the mutant variants Gly100Ala and Gly147Val in conservative loops have been obtained. In this work, the influence of these mutations on stability of PPase globular structure has been studied. Differential scanning calorimetry has been used to determine the apparent enthalpy of thermal denaturation for the native PPase and its mutant variants Gly100Ala and Gly147Val. Guanidine hydrochloride-induced chemical denaturation of PPase has also been studied. It is shown that the substitutions of Gly100 and Gly147 result in overall destabilization of the globular structure.

*Key words*: inorganic pyrophosphatase, globular structure, differential scanning calorimetry, chemical denaturation, energy of denaturation, stability

The soluble inorganic pyrophosphatases (PPases) catalyze hydrolysis of inorganic pyrophosphate ($PP_i$) yielding two phosphates ($P_i$). Family I bacterial PPases including the object of this study function as homohexamers formed by two trimers. The PPase subunit (monomer) is a single-domain protein. Its globule is based on the highly stable hydrophobic core hardly hydrolysable by trypsins. The polypeptide chain of *E. coli* PPase (E-PPase) is folded into a 7-stranded closed β-barrel (Fig. 1). Only noncovalent interactions stabilize the 3D structure of enzyme [1]. The active site is a large cavity with a diameter of about 20 Å with a base supported by the hydrophobic core [2].

The most flexible parts in the structure of *E. coli* PPase are the C-terminus of the polypeptide chain as well as three disordered regions flanking the entry of the active site, hereinafter referred as loops I, II, and III. Conformational flexibility of these regions is partly determined by the invariant glycine residues. Compared to the rest of the amino acid residues, glycine is unique in its structural features. Due to the absence of a side chain, it can provide a high degree of conformational freedom for the polypeptide backbone. In particular, it includes the possibility of "twisting" around the $C_\alpha$-atom of a glycine residue, which in this case acts as a joint. Inclusion of even a single glycine in a segment of a backbone yields a sharp increase in conformational flexibility, especially for short segments. Substitution of glycine with any other residue including alanine should decrease the flexibility of the segment carrying the mutation. Decreasing flexibility not only means the movement of a loop as a whole but the deceleration of switching between the conformations that the residue of this loop can adopt, up to a "freezing" of certain conformation, as well.

Superposition of the crystal structures of *E. coli* PPase and its complexes with a number of ligands shows that in the course of catalysis specific rearrangements of disordered regions I, II, and III take place. The identical movement of these segments in certain stages of catalysis is revealed for the PPases from quite different organisms

*Abbreviations*: PPase) inorganic pyrophosphatase; WT) wild type pyrophosphatase; GuHCl) guanidine hydrochloride.

* To whom correspondence should be addressed.

0006-2979/05/7008-0848 

[1]. Such conservation suggests a certain role for these loops in the functioning of PPases. To clarify the possible role of the loops, it has been proposed to study the properties of enzymes where the flexibility of these segments would be intentionally decreased. To solve this problem, the mutant variants Gly100Ala and Gly147Val of *E. coli* PPase have been prepared with the substitutions in the invariant loops II and III, respectively.

This work was aimed at the study of how the mutations Gly100Ala and Gly147Val influence the stability of the globular structure of *E. coli* PPase. Since both replaced residues are located in conserved elements of secondary structure (β-turns), their mutations could result in a significant destruction of protein structure. Thermal denaturation of the wild-type PPase and the variants Gly100Ala and Gly147Val has been characterized by differential scanning calorimetry. Guanidine hydrochloride (GuHCl)-induced chemical denaturation of the wild-type PPase and the variants Gly100Ala and Gly147Val has also been studied. Such a topic as *in vitro* study of the protein denaturation processes is now of intense interest because of the problem of protein folding *in vivo* and pathways of irreversible aggregation, which are known to cause some neurodegenerative diseases.

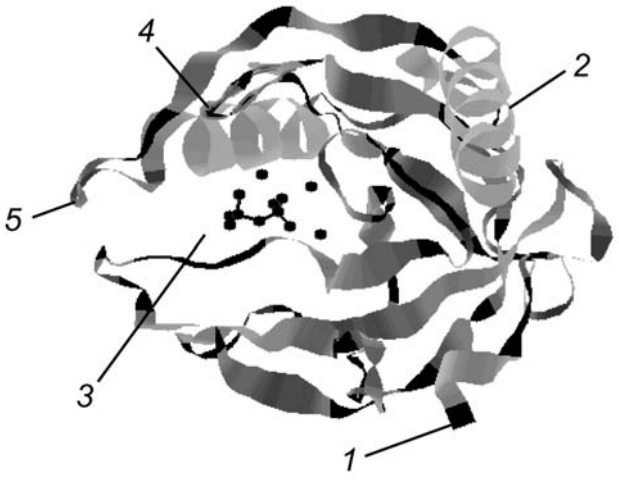


**Fig. 1.** Overall folding of a subunit of *E. coli* PPase. *1*) N-terminus of polypeptide backbone; *2*) C-terminus of backbone; *3*) active site cavity; *4*) loop II; *5*) loop III. Pyrophosphate and three metal ions bound in the active site are shown as ball-and-stick.

## MATERIALS AND METHODS

**Chemicals.** All chemicals used in the work were of highest purity available: Tris, HEPES, $MgCl_2$, NaCl, and methyl green dye from Fluka (Switzerland); guanidine hydrochloride and $Na_4P_2O_7{\cdot}10H_2O$ from Sigma (USA); Triton X-305 from Merck (Germany). Other chemicals were of at least chemical grade. Solutions of $MgCl_2$ were titrated; all stock solutions were freshly prepared using high quality water purified in a MilliQ column.

**Enzyme preparation.** The recombinant *E. coli* inorganic pyrophosphatase and its mutant variants Gly100Ala and Gly147Val were obtained as described previously [2]. Enzyme suspensions were stored in ammonium sulfate at 4°C and desalted before use with a Sephadex G-50 (fine) column equilibrated with 50 mM Tris-HCl, pH 7.5. The concentration of pyrophosphatase solutions was determined by UV-spectroscopy at 280 nm using the specific absorption $A_{280}^{1\%}$ of 11.8 [3].

**Sequence alignment** of the soluble pyrophosphatases was performed using Clustal W software and the BLOSUM weight matrix [4] and additionally corrected considering the structural alignment of *S. cerevisiae* and *E. coli* PPases. Figures 1 and 2 were made using Molscript [5].

**Measurements of hydrolytic activity.** Activities of the wild-type *E. coli* pyrophosphatase and the mutant variants were determined by the rate of $P_i$ release from $MgPP_i$ by quantitative $P_i$ determination using a semiautomatic phosphate analyzer [6]. The enzymatic reaction was carried out with the device sensitivity of 5-10 μM $P_i$ for full-scale. Hydrolysis of $MgPP_i$ was studied in 0.05 M Tris-HCl, pH 7.5, at 25°C. Reaction mixture with total volume of 10 ml contained buffer, 1 mM free $Mg^{2+}$, and 40 μM $MgPP_i$. Hydrolysis was started by an addition of 10-20 μl aliquot of enzyme solution. To calculate total concentrations of magnesium and pyrophosphate to be added, required concentrations of free $Mg^{2+}$ and $MgPP_i$ were preset. All the species containing Mg or $PP_i$ were included into the calculations. Dissociation constants of the corresponding species were used [7]. Mutant variants Gly100Ala and Gly147Val (3-10 mg/ml) were preincubated in 50 mM Tris-HCl, pH 7.5, in the presence of 10 mM $Mg^{2+}$ for 15-20 h at 4°C.

Hydrolytic activities measured after incubation with GuHCl were normalized to the reference value determined after incubation under the same conditions without denaturing agent. The starting values of specific activity were: 500 U/mg (WT PPase), 50 U/mg (Gly100Ala), and 180 U/mg (Gly147Val).

**Differential scanning calorimetry (DSC).** Calorimetric experiments were performed using a differential adiabatic scanning calorimeter DASM-4 (Biopribor, Pushchino, Russia) in platinum capillary cells of volume 0.47 μl. DSC scans were conducted by heating the samples in the temperature range 20-100°C. DSC data were monitored, accumulated, and analyzed using the software specially designed in the Laboratory of Physico-Chemical Methods (Belozersky Institute of Physico-Chemical Biology) and Origin software (MicroCal, USA).

The scan rate was 1.0°C/min unless otherwise stated. Irreversibility of the thermal transitions was assessed by comparing the thermograms obtained in two consec-

utive scans of the same sample. All scans were conducted under the constant excess pressure of 2 atm. Baselines obtained by filling both calorimeter cells with the corresponding buffer (0.1 M HEPES-NaOH, pH 7.5, with or without 10 mM $Mg^{2+}$ depending on the sample) were systematically subtracted from the experimental thermograms.

Before DSC measurements, the proteins were gel filtered using Sephadex G-50 fine column equilibrated with 0.1 M HEPES-NaOH, pH 7.5. The holoform of the wild-type PPase as well as the mutant PPases (in all cases) were additionally preincubated for 15-20 h in the presence of 10 mM $MgCl_2$. In these cases, 10 mM $MgCl_2$ was added to a sample as well as to reference buffer. Enzyme concentrations in the samples were 0.8-1.0 mg/ml (40-50 μM per subunit).

Calorimetric denaturation enthalpy $\Delta H$ was calculated by integration of $\Delta C_p(T)$ across the studied temperature range. The Arrhenius energy of activation of thermal unfolding, $E_a$, was calculated for the model of irreversible, single-step denaturation using Eq. (1) [8]:

$$E_a = eRC_{p,max}T_m^2/\Delta H, \quad (1)$$

where $R$ is the universal gas constant, $C_{p,max}$ is the maximal value of the excess of heat capacity $\Delta C_p$, and $T_m$ is the transition temperature at which $\Delta C_p$ is maximal.

**Chemical denaturation.** Each reaction mixture of volume 0.5 ml contained 50 mM Tris-HCl, pH 7.5, GuHCl of variable concentration (0-8 M), enzyme (0.005-0.5 mg/ml, or 0.25-25 μM per subunit), and, if required, 10 mM $MgCl_2$ or 1 mM $PP_i$. Denaturation mixtures were incubated for 20-24 h at 20-25°C and then PPase activity was measured as described above using 10-20 μl aliquot of each mixture as the source of enzyme.

Residual hydrolytic activity of each PPase normalized by a reference value (namely, activity measured under the same conditions but in the absence of GuHCl) was plotted as a function of GuHCl concentration and analyzed using Eq. (2) [9, 10]:

$$\alpha = \alpha_0 + \frac{Ax^h}{[GuHCl]_{1/2}{}^h + x^h}, \quad (2)$$

where α is fraction of natively folded molecules monitored by normalized PPase activity, $\alpha_0$ is level of the residual activity at high concentrations of GuHCl, $A$ is maximal amplitude of changes in activity, $h$ is the coefficient of cooperativity, $x$ is GuHCl concentration, $[GuHCl]_{1/2}$ is midpoint of transition, i.e., concentration of GuHCl at which the residual activity is half of the starting value.

To determine the oligomeric composition of PPase in the course of denaturation, a series of enzyme solutions of the same concentration (PPase concentration may vary from series to series in the range 0.4-0.6 mg/ml) were incubated for 30-40 h at 25°C in 50 mM Tris-HCl, pH 7.5, in the presence of several fixed concentrations of GuHCl (0-6 M). Analogous experiments were carried out at 6 or 6.5 M GuHCl, and the incubation time was in this case was 3 h. After incubation, each mixture by portions of 100 μl was placed into preliminarily prepared 1 ml spin columns with Sephadex G-50 fine equilibrated with 50 mM Tris-HCl, pH 7.5, and spun for 4 min at 3000 rpm. Eluates from the portions of one sample were mixed together and immediately chromatographed by HPLC.

**HPLC.** Oligomeric forms of the wild-type E-PPase were separated on a TSK Spherogel SW 2000 column using a Beckman HPLC chromatograph (Beckman, USA). The sample of 100 μl was injected and eluted with 50 mM NaCl in 10 mM Tris-HCl, pH 7.5, at a flow rate of 0.5 ml/min. Elution of proteins was monitored by absorption at 280 nm. Retention times for the hexameric and trimeric forms of E-PPase used as markers were 12.7 ± 0.1 min (hexamer, the number of independent measurements, $n = 4$) or 13.9 ± 0.1 min (trimer, $n = 3$). Expected retention time of monomeric form is 15.8 min, and dimeric form 14.6 min. Mean values of the retention times for the main peaks on the experimental elution profiles after incubation with GuHCl were 12.5 ± 0.1 ($n = 8$), 14.08 ± 0.06 ($n = 11$), and 15.6 ± 0.3 ($n = 11$) min. These peaks were identified as hexamer, trimer, and monomer, respectively.

## RESULTS AND DISCUSSION

**Location of residues Gly100 and Gly147 in the structure of *E. coli* PPase.** All three loops flanking the active site cavity in *E. coli* PPase contain catalytically important amino acid residues involved in coordination of activator magnesium ions or substrate. Figure 2 shows the structure of loops II and III discussed in this paper. The short loop II (Fig. 2a) joins the strands β-6 (Val90-Thr96) and β-7 (Asp102-His110) involved in the formation of β-barrel. The residues Asp97 and Asp102, which coordinate $Mg^{2+}$ ions M3 and M1, belong to this segment. Quaternion Asp97-Glu98-Ala99-Gly100 is a β-turn in which the peptide nitrogen atom of Asp97 is H-bonded with the peptide oxygen atom of Gly100 (2.97 Å). Glycine residue Gly100 is the fourth in this quaternion, though in classical β-turns there is a preference for Gly in the third position. In all available structures of *E. coli* PPase, torsion angles φ and ψ of residue Gly100 fall on the Ramachandran plot into fields unallowed for other amino acid residues (φ is always about 125°, ψ is about −150°, with the only exception of the apoform where ψ = −50°). The angle of peptide bond ω for the residues of loop II is close to normal 180° in all structures. The only exception is a structure of the C-subunit in E-PPase complexed with $Mg^{2+}$ (1OBW), which has $Mg^{2+}$ bound only in the subsite

M1. In this structure, ω angles for the peptide bonds immediately preceding and following Gly100 are 146 and 140°, respectively.

Sequence alignment of 90 soluble PPases available in the database shows that only two PPases (both procaryotic) have no Gly residues in the segment homologous to loop II. About one-third of procaryotic PPases as well as all eucaryotic ones contain Gly in the third position of the homologous quaternion rather than in the fourth position. Nineteen PPases contain two or more glycines in the homologous β-turn. In the crystal structures of the only available PPase, where Gly fills the third position of this turn (*Saccharomyces cerevisiae* PPase, e.g., 1E6A), its conformation corresponds to $\alpha_L$ field of the Ramachandran plot. This field is allowed for non-glycine residues, so the glycine in this position of this particular β-turn is not an obligatory condition. Nevertheless, the high conservancy of Gly100 in PPases implies that the insertion in this place of any other residue might cause conformational tension as a result of non-optimal values of torsion

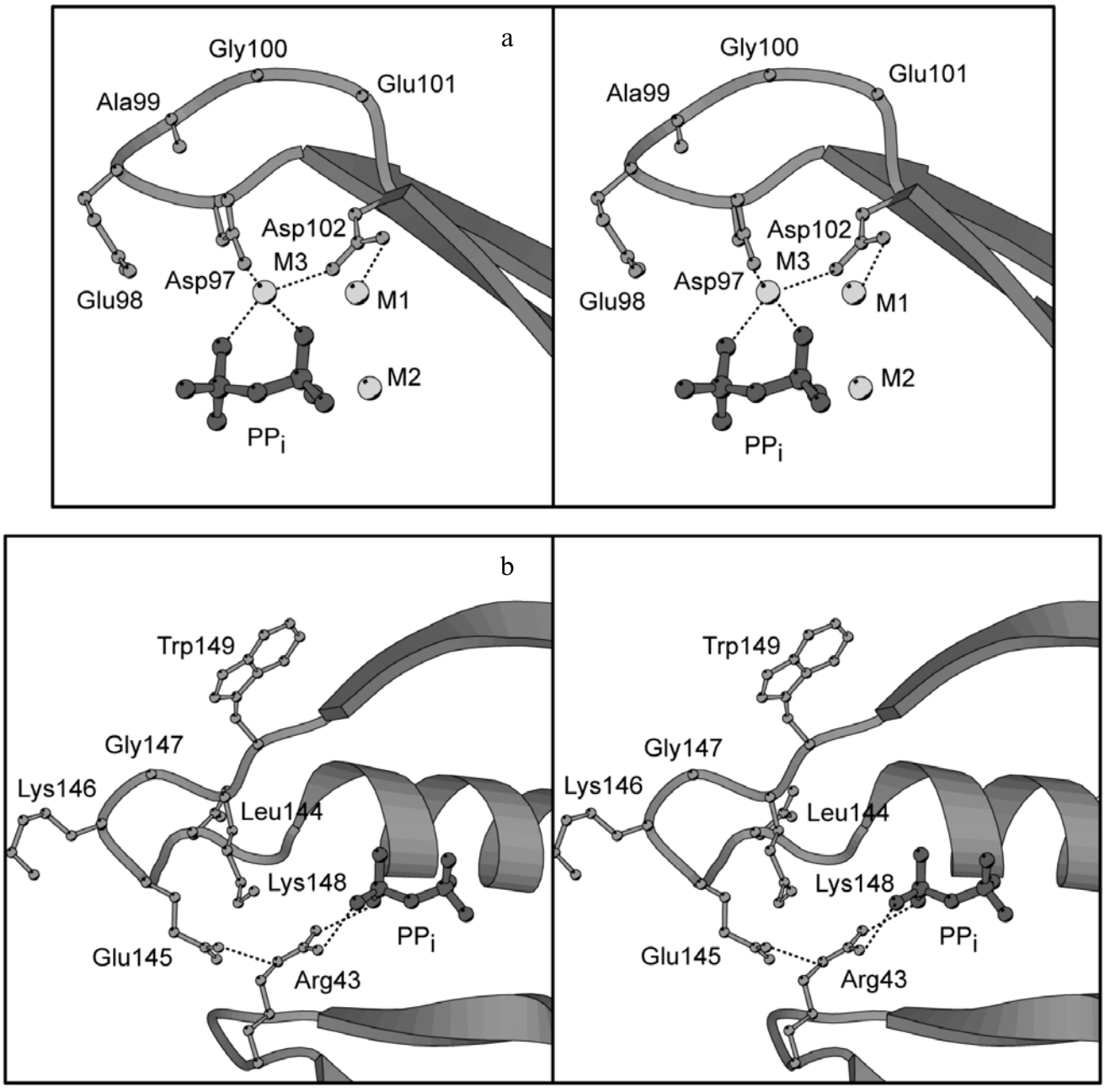


**Fig. 2.** Stereo view of loops II (a) and III (b) and the nearby structural elements. Dashed lines show ionic contacts of the amino acid residues of the loops with the activator metal ions or with the active site residues.

angles and, as a consequence, destabilize the globular structure of the PPase.

Segment III containing Gly147 is a more extended loop joining α-helix A (Glu128-His140) with the strand β-8 (Val150-Glu156, Fig. 2b). Helix A plays an important role in the inter-subunit interface. The residues Tyr141 and Lys142 involved in binding of a pyrophosphate moiety of the substrate are also located in this region. Loop III is built as another structural element of this sort (α-turn-β). Amino acid residues at the C-terminus of the helix still have $\alpha_R$-conformation, but intra-helical H-bonds are not typical for them, and this segment (His140-Leu144) is significantly disordered. Following this helix is β-turn (Glu145-Lys146-Gly147-Lys148) with the H-bond Glu145O–Lys148N (3.13 Å). The residues involved in this loop starting from Glu145 have values of φ and ψ typical for β-strand, except for residue Gly147. Torsion angles of Gly147 vary greatly depending on what ligands are bound in the active site of E-PPase. In the structures of apo-enzyme (1IGP) or E-PPase complexed with the non-hydrolyzable substrate analog $CaPP_i$ (1I6T), Gly147 has positive values of φ and usually adopts a conformation from the non-allowed field of the Ramachandran plot. In the structures of E-PPase complexed with activator magnesium ions (1OBW, 1IPW), this residue has $\alpha_R$-conformation.

In contrast to Gly100, the residue Gly147 is not highly conservative in different PPases. Approximately 30% of sequences (28 PPases) do not have glycine at all in the segment homologous to loop III. The most commonly encountered quaternion in the homologous β-turn of such PPases (Glu-Pro-Asn-Lys) includes a proline residue instead of glycine in the second position. In some cases, the triad Glu-Lys-Lys displaces the quaternion starting from Glu145, and the loop seems to adopt a different conformation. In the PPases where the homologous glycine is still found the conformation of this loop may also differ from E-PPase. A good example is *S. cerevisiae* PPase where, instead of a β-turn starting from Asp196 (homologous to Glu145), a $\pi_{\alpha L}$-turn Lys193-Lys198 is found with H-bonds Lys193O–Lys198N and Ile194O–Gly197N (classical Shellman motif with the Gly residue in the fifth position adopting $\alpha_L$-conformation). In this case, the turn includes a proline residue inside and two more flanking prolines. The residues involved in π-turn in *S. cerevisiae* PPase adopt significantly different conformations compared to the residues of loop III in E-PPase. Thus, a longer loop provides more possibilities for conformational freedom, and the PPases may achieve this freedom in a variety of ways. In addition, in *E. coli* PPase the strand β-8 (Val150-Glu156) is a boundary strand of a β-sheet, and the following is only C-terminal α-helix that does not play any known role in the functioning of this enzyme. From this consideration, one should expect that mutation of Gly147 would not affect the folding and stability of PPase as much as the mutation of Gly100.

It should be noted that in *E. coli* PPase the discussed segments are interconnected. First, the antiparallel strands β-6 (Val90–Thr96) and β-8 (Val150–Glu156) are H-bonded as the nearby strands of a β-barrel. Then, the side chain of Trp149 (the residue next to loop III) has a hydrophobic contact with the $C_\beta$-atom of Glu98. Finally, the side chains of the residues Lys148 and Glu98 form an ion pair in several E-PPase structures.

**Thermal denaturation.** Differential scanning calorimetry has been used to determine the apparent parameters of thermal unfolding of the wild-type E-PPase and the mutant variants Gly100Ala and Gly147Val [11]. The proteins were heated in the temperature range 20-100°C, and DSC trace as a function $\Delta C_p(T)$ was monitored. Since in the kinetic experiments Gly100Ala and Gly147Val PPases were preincubated with 10 mM $Mg^{2+}$, in the thermal unfolding experiments both the wild-type enzyme and the mutant proteins were preincubated at the same magnesium concentration before heating to obtain holoforms. During denaturation itself, the protein solutions also contained 10 mM $Mg^{2+}$. For comparison, the apoform of the wild-type enzyme has been studied. In this case, PPase was not preincubated and the denaturation was performed in the absence of $Mg^{2+}$.

The reversibility of the thermal unfolding of wild-type *E. coli* PPase and the mutant variants was tested by re-heating of the samples. In all cases, only the baseline was reproduced, indicating irreversible denaturation. All the proteins had typical thermograms with well-defined peaks (Fig. 3). Determined from these peaks, the value of $T_m$ (temperature of the maximal heat capacity), $\Delta H$ (calorimetric enthalpy), and $E_a$ (activation energy of unfolding) are collected in Table 1.

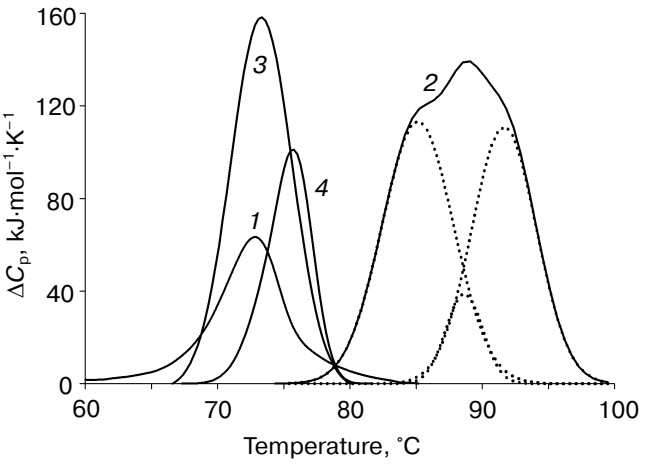


**Fig. 3.** Differential scanning calorimetry of the wild-type *E. coli* PPase and the mutant variants: *1*) apoform of the wild-type E-PPase; *2*) holoform of PPase (10 mM $Mg^{2+}$); *3*) mutant variant Gly100Ala (10 mM $Mg^{2+}$); *4*) mutant variant Gly147Val (10 mM $Mg^{2+}$). Conditions: 0.1 M Hepes-NaOH, pH 7.5. Solid lines are the continuous monitoring of $\Delta C_p$ signal. The dotted line is the best fit of thermogram *2* (see text).

**Table 1.** Parameters of the thermal unfolding of the wild-type *E. coli* PPase and the mutant variants Gly100Ala and Gly147Val

| E-PPase | $T_m$, °C | $\Delta H$, kJ/mol | $E_a$, kJ/mol* | $k$, °C** |
|---|---|---|---|---|
| WT, apoform | 72.8 | 440 | 17.3 | 4.7 |
| WT, 10 mM $Mg^{2+}$*** | 85.6<br>88.1<br>91.7 | 1580 | | 5.4<br>2.7<br>4.8 |
| Gly100Ala, 10 mM $Mg^{2+}$ | 73.3 | 940 | 20.5 | 4.65 |
| Gly147Val, 10 mM $Mg^{2+}$ | 75.7 | 430 | 30.6 | 4.5 |

* The values are calculated by formula (1) for one-stage irreversible denaturation.
** Parameter characterizing the peak width at the half of its height.
*** The $T_m$ values calculated from processing the melting curve as the sum of three peaks are provided.

The apoform of the wild-type E-PPase is characterized by a high melting point ($T_m$ = 73°C) and high cooperativity (judged from low value of $k$ determined as peak width at its half-height). Changing PPase concentration in the range 0.5-2.0 mg/ml did not greatly alter the apparent parameters $T_m$ and $\Delta H$. This indicates that the unfolding of the apoform of E-PPase can be described by a simple two-state model [8]. $T_m$ and $\Delta H$ were virtually unaffected by variation of the scan rate in the range 0.25-1.0°C/min as well. According to [8], deviation from a monomolecular mechanism of the denaturation might be a possible reason for this observation; on the other hand, the limited precision of the determination of experimental parameters does not allow a final conclusion.

The addition of 10 mM $Mg^{2+}$ results in an increase in $T_m$ of more than 10°C, denaturation enthalpy for the holoform increases threefold, and its thermogram is complex. The increase in $T_m$ and $\Delta H$ for the holoform is quite reasonable because the stabilizing effect of $Mg^{2+}$ on the structure of PPase is well known [12]. $Mg^{2+}$ has four binding subsites within the active site of each subunit of PPase and, in addition, can occupy a binding site in the intertrimeric interface. Superposition of the spatial structures of the apoform of E-PPase and its complex with $Mg^{2+}$ shows that the binding of the first metal ion still causes significant ordering of the structure, and a great number of new noncovalent interactions between residues are formed [12]. Another evident difference in the denaturation curves for the apo- and the holoform of the wild-type PPase does not have so clear reason. The melting peak of the apoenzyme is symmetrical, whereas for the holoform the curve splits into overlapped peaks (Fig. 3). The most accurate description of this curve is given by a sum of three Gaussian peaks, two of which correspond to the main maxima with $T_m$ 85.6 and 91.7°C, and the third one corresponds to a minor maximum with $T_m$ 88.1°C. Since denaturation of PPase is irreversible, this resolution of a total curve into three constituents is given only for visual evidence. To quantitatively compare parameters of denaturation with the other forms, we used the total area under the peak yielding the value of calorimetric enthalpy $\Delta H$ = 1580 kJ/mol (Table 1). This complex character of the thermogram indicates that the denaturation of the holoform of PPase cannot be described within the simplest two-state model because the path from the completely folded protein to completely unfolded one includes certain thermodynamically stable intermediates. Several peaks on the curve cannot be easily attributed to the sequential unfolding of the different parts of a globule, as in other cases of that sort, since the PPase molecule is single-domain. Maxima with different $T_m$ cannot also be explained by separate unfolding of various oligomeric forms of E-PPase, since the presence of $Mg^{2+}$ and the high protein concentration in the experiment obviously rules out the possibility of dissociation of the hexamer in the course of the DSC experiment. Perhaps some conformers are stabilized in the holoform of PPase so that transitions between them are slow on the DSC time scale for some reason or other. This conformational heterogeneity of the PPase solution might explain the observed complex thermogram of the holoform.

The studied mutant PPases show cooperative denaturation, and their thermograms do not display any additional peaks. Mutations of either residue Gly100 or Gly147 result in a decrease of the melting point by about 20°C compared to the holoform of the wild-type PPase, and in a significant decrease in the denaturation enthalpy (Table 1). Since in the course of the thermal unfolding noncovalent interactions are destroyed in the whole volume of the globule, this difference indicates the total destabilization of the spatial structure of E-PPase. The observed decline in $\Delta H$ may also be interpreted as an increase in the energy costs for the reverse process of PPase folding in the course of its biosynthesis. The folding process often follows the same pathway, includes the same intermediates, and is characterized by the same

magnitude of $\Delta G_{den}(H_2O)$ as unfolding [13]. Therefore, the destabilization of the mutant PPases indicates that residues Gly100 and Gly147 play a definite role for the quick and correct folding of PPase into the native structure.

The fact that the holoforms of both mutant variants Gly100Ala and Gly147Val, in contrast to the wild-type E-PPase, display simple thermograms with a single maximum might be explained by the existence of only one stable conformation in their solutions. This fact may also be related with extremely slow transitions in the mutant PPases, up to arresting certain conformations from the whole population. This last consideration seems rather reasonable since catalytically important conformational transitions for the variants Gly100 and Gly147 are known to take at least 10-20 h.

**Chemical denaturation.** *Determination of* $[GuHCl]_{1/2}$. The effect of the mutations Gly100Ala and Gly147Val on the stability of E-PPase with respect to a chemical denaturation has been investigated in this work. Guanidine hydrochloride (GuHCl) was used as a denaturant, since another commonly used agent, urea, did not promote PPase unfolding. Catalytic activity of the wild-type E-PPase is decreased by the action of GuHCl reaching a constant non-zero level after 15-18 h at 2-4 M GuHCl, 10-12 h at 5 M GuHCl, or 2-4 h at 7 M GuHCl. The residual activity does not change further for up to 80 h. Since the enzyme is catalytically active only in the properly folded state, one can expect that the decline in activity correlates with the decrease in the fraction of natively folded protein molecules. To determine the profile of equilibrium denaturation, the wild-type PPase and the mutant variants were incubated in the presence of GuHCl for 20-24 h and then the residual activity was measured. Since the mutant PPases Gly100Ala and Gly147Val are catalytically active only after preincubation with $Mg^{2+}$, the reaction mixtures for the denaturation of the studied proteins unless otherwise stated contained 10 mM $MgCl_2$.

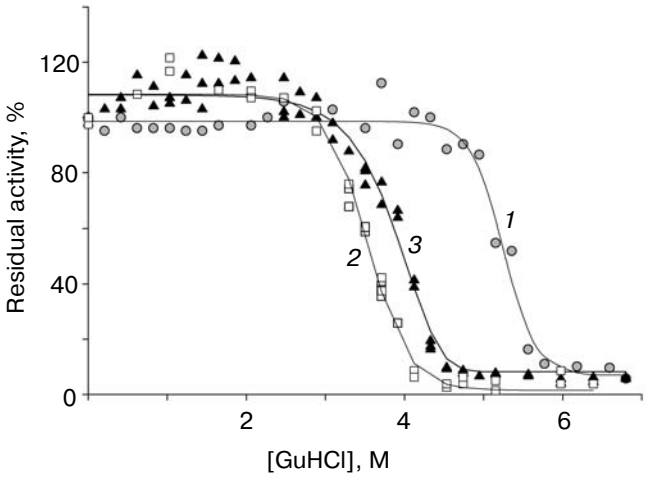


**Fig. 4.** Residual activity of the native PPase (*1*) and its mutant variants Gly100Ala (*2*) and Gly147Val (*3*) after incubation with GuHCl. Conditions of denaturation: 0.5 M Tris-HCl, pH 7.5, 10 mM $MgCl_2$, enzyme concentrations 0.1 mg/ml (*1*, *3*) or 0.5 mg/ml (*2*). All enzymes were preincubated with 10 mM $Mg^{2+}$. Lines are the best fit of Eq. (2) to the experimental data.

**Table 2.** GuHCl-induced denaturation of the wild-type PPase and the mutant variants Gly100Ala and Gly147Val (50 mM Tris-HCl, pH 7.5; enzyme concentrations: 0.1 mg/ml (WT PPase and Gly147Val) or 0.5 mg/ml (Gly100Ala))

| PPase | Ligands | $[GuHCl]_{1/2}$, M |
|---|---|---|
| WT | — | 4.5 |
| | 10 mM $Mg^{2+}$ | 5.3 |
| | 1 mM $PP_i$ | 4.4 |
| WT [18]* | — | 4.5 |
| | 5 mM $Mg^{2+}$ | 4.9 |
| G100A | 10 mM $Mg^{2+}$ | 3.6 |
| G147V | 10 mM $Mg^{2+}$ | 3.9 |

* 20 mM Tris-HCl, pH 7.0; enzyme concentration 0.04 mg/ml.

Figure 4 presents the residual activity (normalized for the reference value) as a function of GuHCl concentration. Classical sigmoidal dependence with high cooperativity of transition from the native to unfolded state can be observed for all three PPases. Treatment of the experimental data by Eq. (2) enables the calculation of a midpoint of transition, $[GuHCl]_{1/2}$.

The wild-type PPase has a rather high value of $[GuHCl]_{1/2}$. For the apoform of PPase the midpoint is 4.5 M, and for the holoform (in the presence of 10 mM $Mg^{2+}$) this value is still higher (5.3 M, Table 2). For comparison, many proteins are characterized by midpoints of about 3 M [14-16]. E-PPase retains some residual activity even after incubation in 8 M GuHCl.

*Characteristics of the denatured state.* The absence of additional plateaus on the denaturation profile is consistent with the approximation of the unfolding of PPases as a simple two-state transition from the native to the unfolded state without any thermodynamic intermediates. At any given GuHCl concentration, only the native (N) and unfolded (U) states of a protein molecule comprise a significant population.

E-PPase and the mutant variants Gly100Ala and Gly147Val exist under the usual conditions as homohexamers. Any other oligomeric forms of these PPases cannot be obtained at pH 7.5 and 10 mM $Mg^{2+}$. To get trimeric enzyme, hexamer should be incubated at pH 4-5, and a dimeric form can be obtained by addition to the protein solution of organic solvent, e.g., isopropanol [17]. The

monomeric form of E-PPase is quite unstable and has a tendency for irreversible aggregation. Nevertheless, the chemical denaturant might facilitate the destruction of inter-subunit contacts, so the oligomeric nature of the denatured state U of E-PPase is not unequivocal. If the quaternary structure is impaired together with the tertiary structure (this phenomenon is found for a variety of small globular proteins), the denatured state of E-PPase may be populated by monomers, dimers, or trimers.

According to literature data [18], inorganic pyrophosphatase from *Sulfolobus acidocaldarius* that has a high homology with E-PPase and is also hexameric in solution can dissociate to monomers under the influence of GuHCl. The most substantial changes in the secondary and tertiary structure of this PPase occur in the same range of GuHCl concentrations as the dissociation, as judged from CD- and fluorescence spectroscopy.

In this work, the shift in oligomeric composition of *E. coli* PPase upon denaturation was investigated by HPLC. The wild-type enzyme at a concentration of 0.6 mg/ml (30 μM) was incubated for 30-40 h in the presence of GuHCl of variable concentration followed by a fast separation of denaturant and HPLC of the resulting mixture. The experimental data (Fig. 5) show that the hexameric E-PPase (retention time 12.5 min) in the course of denaturation dissociates with the simultaneous formation of trimers (retention time range 14.2-14.5 min) and monomers (15.5-16.0 min). The peaks of various oligomeric forms broaden as GuHCl concentration is increased, probably indicating a change in compactness of the protein globule dependent on the degree of denaturation. Trimers and monomers start forming at 4 M GuHCl, but there is still a significant population of trimer in the mixture at 6 M denaturant. Some amount of aggregated protein is also accumulated in the mixture (retention time 9.3 min). These results do not allow exact determination of the relative amounts of the oligomeric forms of E-PPase since: a) the separate peaks start broadening and overlapping as a result of denaturation, and b) reassociation of trimers into hexamers (and/or monomers into trimers) after separation of denaturant cannot be excluded. Nevertheless, these data clearly demonstrate that after incubation in the presence of GuHCl the hexameric E-PPase partly dissociates. As reported for the *S. acidocaldarius* PPase [18], dissociation is observed in the same range of GuHCl concentrations as denaturation. Dissociation of E-PPase at lower concentrations of GuHCl is also possible as shown below, but the formation of trimers in this case becomes evident only at lower protein concentration.

Thus, denaturation of E-PPase occurs in fact through a complicated mechanism involving formation of intermediates of various oligomeric states and in various degrees of denaturation.

*Stability of the mutant variants Gly100Ala and Gly147Val.* Denaturation profiles of the mutant enzymes

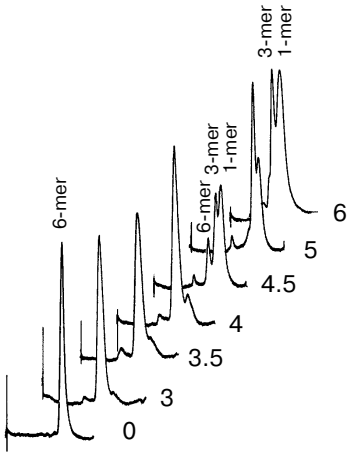


| [GuHCl], M | 6-mer | 3-mer | 1-mer |
|---|---|---|---|
| 6 | – | 14.1 | 15.7 |
| 5 | – | 14.2 | 15.5 |
| 4.5 | 12.7 | 14.2 | 15.5 |
| 4 | 12.8 | – | 16.1 |
| 3.5 | 13.0 | – | 16.0 |
| 3 | 12.8 | – | 16.0 |
| 0 | 12.7 | – | – |

**Fig. 5.** HPLC elution profiles of the wild-type PPase after incubation with GuHCl followed by a fast separation of the denaturant. Concentrations of GuHCl (M) are shown on the profiles. Retention times of the main peaks (min) are given separately.

Gly100Ala and Gly147Val are similar to that for the wild-type E-PPase. The value of $[GuHCl]_{1/2}$ is however significantly lower for either mutant PPase than for the native enzyme (Table 2) indicating the destabilizing effect of mutation of residues Gly100 and Gly147. Though the decrease in $[GuHCl]_{1/2}$ is itself neither a necessary nor a sufficient condition to exactly state that the mutations destabilize globular structure, the estimated magnitude of denaturation energy for the wild-type and the mutant PPases (data not shown) supports this conclusion.

Thus, both mutations appear to facilitate chemical denaturation. Since loops II and III containing the mutated residues are arranged on the surface of the PPase globule, the chemical denaturation is thought to reflect mainly a contribution of these loops in the primary interaction of the protein with GuHCl. Easier denaturation of the mutant PPases may be therefore regarded under the assumption that, as a result of mutation, the conformation of loops II and III may be distorted due to non-optimal torsion angles, and the loops may move from the surface diminishing the number of protein contacts and thereby facilitating approach of denaturant to the protein surface.

It should be noted that at GuHCl concentrations below 2 M activation of mutant PPases is clearly evident (Fig. 4). This observation may be explained by the possibility that an early unfolding of the surface elements including loops II and III facilitates the conformational transitions yielding faster hydrolysis.

*Denaturation of the PPases at low enzyme concentration.* The two-state model is applicable for the denaturation of E-PPase and the mutant variants Gly100Ala and Gly147Val only if the protein concentration during the incubation with GuHCl is high enough (at least, 0.1 mg/ml or 5 μM per subunit). At lower protein con-

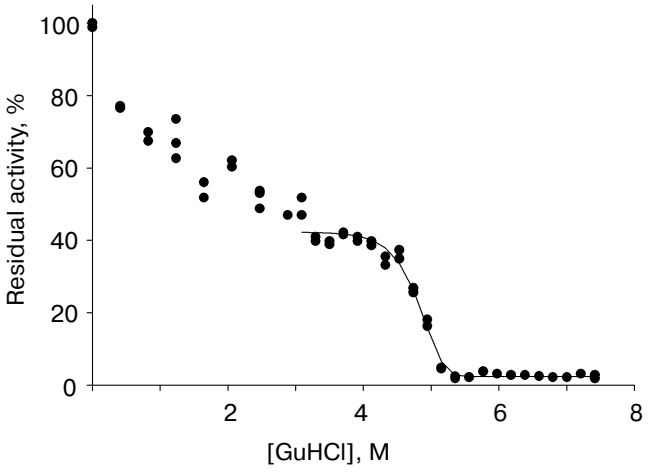


**Fig. 6.** Residual activity of the wild-type E-PPase after incubation with GuHCl. Enzyme concentration 0.005 mg/ml. The line is the best fit of Eq. (2) to the experimental data, starting from 3 M GuHCl.

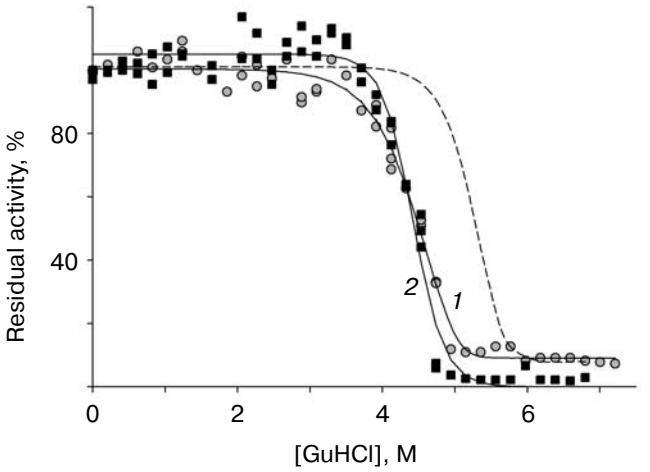


**Fig. 7.** Residual activity of the apoform of wild-type E-PPase (*1*) and its complex with 1 mM $PP_i$ (*2*) after incubation with GuHCl. Conditions: 0.5 M Tris-HCl, pH 7.5, enzyme concentration 0.1 mg/ml. The lines are the best fit of Eq. (2) to the experimental data. For comparison, the denaturation profile for the holoform of PPase (10 mM $MgCl_2$) is shown by a dashed line.

centrations, the denaturation curve splits into two segments (Fig. 6). Increasing GuHCl concentration up to 4 M is accompanied with the gradual decrease in PPase activity, its value finally reaching 40-50% level typical for the trimer [17]. Further increasing of GuHCl concentration yields a sharp sigmoidal decline in activity with midpoint similar to the hexameric form of PPase. The first stage of this dependence may be supposed to reflect the reversible dissociation of the protein into trimers. HPLC data of the enzyme samples of the higher concentration (Fig. 5) show that GuHCl can indeed provoke dissociation of the hexameric PPase into trimers at pH 7.5. For the lower protein concentrations, the hexamer ↔ trimer equilibrium appears to shift toward trimer at moderate concentrations of GuHCl not sufficient for denaturation, and the trimer thereby formed denatures cooperatively at GuHCl concentrations higher than 4 M.

*Effect of metal-free pyrophosphate on the stability of PPase.* In contrast to magnesium pyrophosphate, metal-free pyrophosphate is not a substrate of PPase but is capable of binding at the effector site of PPase and activating hydrolysis of $MgPP_i$ [19, 20]. The location of the effector site in the PPase structure has not been yet determined, nor the mechanism of activation clarified. Allosteric activation of PPase implies that the structure of the enzyme alters in response to the binding of metal-free $PP_i$. To clarify in what way the action of effector may be connected with the conformational flexibility of the globule, we investigated denaturation of the wild-type enzyme in the presence of 1 mM metal-free $PP_i$ (Table 2). As can be seen from Fig. 7, parameter $[GuHCl]_{1/2}$ was not greatly affected by the presence of effector. On the other hand, the energy of denaturation estimated within the two-state model rose sharply compared to the apoform (data not shown). Perhaps, stabilization of the structure invoked by effector resulted from formation of new contacts between the surface elements not bound in the apoform. An alternative possibility is that the structural rearrangements after $PP_i$ binding cause the burial of the hydrophobic patterns of the globule that are exposed to solvent in the apoform, so that the change in the total hydrophobic area accompanying GuHCl-induced denaturation is higher in the case of enzyme–$PP_i$ complex. In some way, binding of effector considerably stabilizes the PPase globule.

It should be noted that, in contrast to the action of metal-free $PP_i$, stabilizing effect of $Mg^{2+}$ is accompanied by a significant increase in the unfolding midpoint $[GuHCl]_{1/2}$. One of the possible reasons for this finding is that the fraction of natively folded molecules was monitored by catalytic activity. Magnesium ions binding in the active site cavity inside the globule stabilize mainly the protein core, so the high level of activity is retained up to higher concentrations of denaturing agent in spite of partial unfolding of the surface elements. Under this assumption, metal-free $PP_i$ is bound in such a way that it forces stronger fixation of certain surface elements. At first, such a fixation results in labored denaturation, but when the surface loops eventually unfold the remainder of a structure denatures with a high degree of cooperativity.

This work was carried out under financial assistance of the Russian Foundation for Basic Research (grant Nos. 03-04-48866 and 1706-2003-4).

## REFERENCES


1. Rodina, E. V. (2003) in *Protein Structures: Kaleidoscope of Structural Properties and Functions* (Uversky, V. N., ed.) Research Signpost, Kerala, India, pp. 627-650.
2. Oganessyan, V. Yu., Kurilova, S. A., Vorobyeva, N. N., Nazarova, T. I., Popov, A. N., Lebedev, A. A., Avaeva, S. M., and Harutyunyan, E. H. (1994) *FEBS Lett.*, **348**, 301-304.
3. Josse, J. (1966) *J. Biol. Chem.*, **241**, 1938-1947.
4. Thompson, J. D., Higgins, D. G., and Gibson, T. J. (1994) *Nucleic Acids Res.*, **22**, 4673-4680.
5. Kraulis, P. (1991) *J. Appl. Crystallogr.*, **24**, 946-950.
6. Baykov, A. A., and Avaeva, S. M. (1981) *Analyt. Biochem.*, **116**, 1-4.
7. Shafranskii, Iu. A., Baykov, A. A., Andrukovich, P. F., and Avaeva, S. M. (1977) *Biokhimiya*, **42**, 1244-1254.
8. Lyubarev, A. E., and Kurganov, B. I. (2000) *Uspekhi Biol. Khim.*, **40**, 43-84.
9. Tanford, C. (1970) *Adv. Prot. Chem.*, **24**, 1-95.
10. Pace, C. N. (1986) *Meth. Enzymol.*, **131**, 266-279.
11. Privalov, P. L. (1979) *Adv. Prot. Chem.*, **33**, 167-241.
12. Avaeva, S. M., Rodina, E. V., Vorobyeva, N. N., Kurilova, S. A., Nazarova, T. I., Sklyankina, V. A., Oganessyan, V. Y., and Harutyunyan, E. G. (1998) *Biochemistry (Moscow)*, **63**, 592-599.
13. Rietveld, A. W., and Ferreira, S. T. (1998) *Biochemistry*, **37**, 933-937.
14. Millet, I. S., Townsley, L. E., Chiti, F., Doniach, S., and Plaxco, K. W. (2002) *Biochemistry*, **41**, 321-325.
15. Del Vecchio, P., Graziano, G., Granata, V., Barone, G., Mandrich, L., Manco, G., and Rossi, M. (2002) *Biochemistry*, **41**, 1364-1371.
16. Morgan, C. J., Wilkins, D. K., Smith, L. J., Kawata, Y., and Dobson, C. M. (2000) *J. Mol. Biol.*, **300**, 11-16.
17. Vainonen, J. P., Kurilova, S. A., and Avaeva, S. M. (2002) *Bioorg. Khim.*, **28**, 426-433.
18. Hansen, T., Urbanke, C., Leppanen, V.-M., Goldman, A., Brandenburg, K., and Schafer, G. (1999) *Arch. Biochem. Biophys.*, **363**, 135-147.
19. Sitnik, T. S., Vainonen, J. P., Rodina, E. V., Nazarova, T. I., Kurilova, S. A., Vorobyeva, N. N., and Avaeva, S. M. (2003) *Life*, **55**, 37-41.
20. Vainonen, J. P. (2002) *Obtaining and Studying of Different Oligomeric Forms of Escherichia coli Inorganic Pyrophosphatase. Activation by Pyrophosphate*: Author's abstract of Candidate's dissertation [in Russian], Moscow State University, Moscow.